Global Change Biology

Global Change Biology (2015) **21**, 3520–3531, doi: 10.1111/gcb.12945

Time-lag effects of global vegetation responses to climate change

DONGHAI WU[1,2], XIANG ZHAO[1], SHUNLIN LIANG[1,3], TAO ZHOU[4,5], KAICHENG HUANG[4,5], BIJIAN TANG[1,2] and WENQIAN ZHAO[1,2]

[1]*The State Key Laboratory of Remote Sensing Science, School of Geography, Beijing Normal University, Beijing 100875, China,* [2]*College of Global Change and Earth System Sciences, Beijing Normal University, Beijing 100875, China,* [3]*Department of Geographical Sciences, University of Maryland, College Park, MD 20742, USA,* [4]*State Key Laboratory of Earth Surface Processes and Resource Ecology, Beijing Normal University, Beijing 100875, China,* [5]*Academy of Disaster Reduction and Emergency Management, Ministry of Civil Affairs and Ministry of Education, Beijing 100875, China*

Abstract

Climate conditions significantly affect vegetation growth in terrestrial ecosystems. Due to the spatial heterogeneity of ecosystems, the vegetation responses to climate vary considerably with the diverse spatial patterns and the time-lag effects, which are the most important mechanism of climate–vegetation interactive effects. Extensive studies focused on large-scale vegetation–climate interactions use the simultaneous meteorological and vegetation indicators to develop models; however, the time-lag effects are less considered, which tends to increase uncertainty. In this study, we aim to quantitatively determine the time-lag effects of global vegetation responses to different climatic factors using the GIMMS3g NDVI time series and the CRU temperature, precipitation, and solar radiation datasets. First, this study analyzed the time-lag effects of global vegetation responses to different climatic factors. Then, a multiple linear regression model and partial correlation model were established to statistically analyze the roles of different climatic factors on vegetation responses, from which the primary climate-driving factors for different vegetation types were determined. The results showed that (i) both the time-lag effects of the vegetation responses and the major climate-driving factors that significantly affect vegetation growth varied significantly at the global scale, which was related to the diverse vegetation and climate characteristics; (ii) regarding the time-lag effects, the climatic factors explained 64% variation of the global vegetation growth, which was 11% relatively higher than the model ignoring the time-lag effects; (iii) for the area with a significant change trend (for the period 1982–2008) in the global GIMMS3g NDVI ($P < 0.05$), the primary driving factor was temperature; and (iv) at the regional scale, the variation in vegetation growth was also related to human activities and natural disturbances. Considering the time-lag effects is quite important for better predicting and evaluating the vegetation dynamics under the background of global climate change.

Keywords: climate change, GIMMS3g NDVI, precipitation, solar radiation, temperature, time-lag effects, vegetation growth

Received 26 January 2015 and accepted 20 March 2015

Introduction

Global climate change has significantly impacted terrestrial ecosystems over the past century (Walther *et al.*, 2002; Kelly & Goulden, 2008; Reichstein *et al.*, 2013; Zhou *et al.*, 2014); therefore, it is particularly important to investigate the spatial and temporal patterns of the ecosystem's responses to climate. Global warming leads to a more frequent occurrence of extreme weather and climatic events, such as extreme heat, precipitation, and drought, which have significant impacts on ecosystems at different spatiotemporal scales (Easterling *et al.*, 2000; Karl & Trenberth, 2003; Kumar, 2013; Zhang *et al.*, 2014). For example, the extreme droughts in the Amazon in 2005 and 2010 caused widespread mortality of trees (Marengo *et al.*, 2008; Lewis *et al.*, 2011; Xu *et al.*, 2011). Simultaneously, global warming also has a positive effect on vegetation growth, especially for ecosystems at high latitudes where the temperature is a major limiting factor. The warming climate enhances vegetation photosynthesis and extends the length of the growing season by advancing its initiation and delaying its termination (Jeong *et al.*, 2011). The impacts of climate change on the global carbon cycle resulted in an increase in the global NPP (net primary productivity) in 1982–1999 of 3.4 Pg C and a decreased of 0.55 Pg C in 2000–2009 (Nemani *et al.*, 2003; Zhao & Running, 2010).

In general, vegetation growth primarily depends on external climatic factors: temperature, precipitation, and radiation (Bonan, 2008; Beer *et al.*, 2010; Wang *et al.*, 2011; Craine *et al.*, 2012). The dominant factors are radiation in the rainforest, precipitation in arid and semiarid areas, and temperature at high northern

Correspondence: Xiang Zhao, tel. +86 10 5880 3001; fax +86 10 5880 3001, e-mail: zhaoxiang@bnu.edu.cn

latitudes (Nemani *et al.*, 2003). Jong *et al.* (2013) described the relationship between vegetation and climate based on meteorological indicators and analyzed the impacts of climatic factors on the variations of vegetation growth over the past 30 years; the results showed that climate could explain approximately 54% of the variation in vegetation. However, the aforementioned studies primarily focused on the impacts of the simultaneous climatic factors and did not consider the time-lag effects of climatic factors on vegetation growth.

Recently, increasing studies have found that the responses of vegetation to climate have a certain time lag (Davis, 1989; Kuzyakov & Gavrichkova, 2010; Vicente-Serrano *et al.*, 2012; Saatchi *et al.*, 2013; Chen *et al.*, 2014; Rammig *et al.*, 2014). Braswell *et al.* (1997) investigated the interannual lag of vegetation's response to temperature and found differences in the time-lag effects among different ecosystems. The controlled experiments showed that an extreme climatic event (i.e., heat) in a grassland ecosystem in a certain year would cause a decrease in NEP (net ecosystem productivity) in the current and following years, with a time lag of 2 years (Arnone Iii *et al.*, 2008). Studies performed at the regional scale, which commonly adopted remote sensing data, also found a time-lag effect. For example, Anderson *et al.* (2010) investigated the time-lag effects for different climatic factors (i.e., radiation, rainfall, and aerosol optical depth) in the Amazon and found that the time lag of the vegetation responses to climatic factors differed in the rainforest. Research on the Australian mainland found that the vegetation responses to soil moisture lagged by approximately one month (Chen *et al.*, 2014). These studies recognize the importance of the time-lag effects of vegetation responses to climate. In other words, vegetation growth may not primarily be driven by present climatic conditions, but earlier climatic conditions may have the most impact on vegetation growth. Therefore, time-lag effects should be considered when exploring the mechanism of climate-vegetation interactive effects.

Although the time-lag effects are extremely important for the impacts of climate on ecosystems, most studies that focused on large-scale climate–vegetation interaction adopted the simultaneous meteorological and vegetation indicators and the time-lag effects were minimally considered (Jong *et al.*, 2013; Peng *et al.*, 2013), which would increase the uncertainty of the results. Because there is still a lack of the spatial patterns for the time-lag effects of vegetation responses to climate at the global scale, we propose that the same type of vegetation may have different time-lag effects to different climatic factors and different vegetation types may respond differently to the same climatic factor. Therefore, we aim to determine the temporal-explicit and spatial-explicit patterns of the vegetation responses to climate.

Based on the NDVI data from the GIMMS3g (Global Inventory Monitoring and Modeling Systems) (Tucker *et al.*, 2005) and the meteorological data from the CRU (Climate Research Unit) (Harris *et al.*, 2014), we first evaluated the statistical relationship between the NDVI and climatic factors (temperature, precipitation, and radiation), considering the possible time-lag effects. First, the study analyzed the time-lag effects of three meteorological factors on the variation of vegetation growth. Based on the revealed time-lag effects, a multiple linear regression model was then established to quantitatively analyze the relationship between the variation of the comprehensive climatic factors and the variation of the vegetation growth. We also established a partial correlation model to determine the roles of different climatic factors on vegetation responses, which were used to determine the driving factors of global vegetation variations from 1982 to 2008.

Materials and methods

Data

Climate data. The monthly temperature and precipitation datasets used in this study were from the Climate Research Unit (CRU), version TS3.21 (Harris *et al.*, 2014), which spanned the twentieth century and, therefore, covered our study period (1982–2008) with a spatial resolution of 0.5°. The gridded datasets were obtained from more than 4000 meteorological stations and interpolated based on spatial autocorrelation functions (New *et al.*, 2000; Mitchell & Jones, 2005). The solar radiation monthly dataset was obtained from the CRU-NCEP V5.2 dataset, with the same spatial resolution as the CRU climate data. This dataset was derived from the combination of the CRU TS3.21 climate dataset (1901–2012) and the NCEP reanalysis, which covered the period 1948–2009. All of the climate datasets were thoroughly evaluated and applied in global climate studies (Wang *et al.*, 2011; Jones *et al.*, 2012; Jong *et al.*, 2013; Peng *et al.*, 2013).

NDVI time series. The Global Inventory Monitoring and Modeling Systems (GIMMS3g) NDVI dataset (Tucker *et al.*, 2005), acquired from the National Oceanographic and Atmospheric Administration (NOAA), with the Advanced Very High-resolution Radiometer (AVHRR), was used for the analysis. This long-time series data spanned from 1982 to 2011 at a spatial resolution of 0.083° and a 15-day interval (Fensholt & Proud, 2012). The maximum value composite (MVC) method was adopted for the fortnightly scenes, which can largely remove atmospheric noise (Holben, 1986). The GIMMS3g NDVI dataset provided the longest time series of approximately three

decades, and it has been widely used for global vegetation monitoring (De Jong *et al.*, 2013; Mao *et al.*, 2013; Peng *et al.*, 2013; Wang *et al.*, 2011; Wu *et al.*, 2014). Data analyses were conducted at a monthly temporal scale; therefore, the MVC method was applied to the biweekly composite data by pixels. Compared with Jong's study, we chose the same time period from 1982 to 2008 for our analysis. We also averaged the global monthly NDVI corresponding to each pixel of the climate dataset to match the GIMMS3g NDVI data with the CRU climate data.

Land-cover data. A collection 5.1 MODIS land-cover product (MCD12C1) was used in this study for statistical analysis (Friedman *et al.*, 2000; Friedl *et al.*, 2010). There were five land-cover classification schemes in this dataset, and the International Geosphere and Biosphere Programme (IGBP), at a spatial resolution of 0.05° from 2001 to 2008, was developed. This dataset consists of 17 general land-cover types, which include 11 natural vegetation classes, three developed and mosaicked land classes and three nonvegetated land classes (Friedl *et al.*, 2002, 2010).

The unchanged vegetation type map, shown in Fig. 1, was derived from the MCD12C1. An unchanged pixel is defined as a pixel always being the same vegetation type during the period 2001–2008. Open shrublands were divided into two types, one distributed at high latitudes and the other in middle and lower latitudes, as each has very different climate conditions. To diminish the impacts of land-cover changes caused by natural and human disturbances, only the grids that have the unchanged vegetation type were used to analyze spatial patterns and the time-lag effects of vegetation responses to climate. At a 0.5 spatial resolution, all statistic samples in this study extracted the subpixel frequency of one vegetation type more than 90%. Samples of one vegetation type for which there were more than 50 counts were considered in the analysis, and there were 12 types chosen in the statistics, which are shown in Table 1.

Methods

In this study, the analysis of vegetation responses to climate (i.e., temperature, precipitation and radiation) was performed at the global scale in four aspects: (i) the time-lag effects of vegetation responses to climatic factors, (ii) the overall explanation of climatic factors on vegetation growth, (iii) the major climate-driving factors on vegetation variation, and (iv) the climate-driving factors of significant vegetation variation ($P < 0.05$) globally for the period 1982–2008.

Time-lag effects of vegetation responses to climatic factors

The temperature, precipitation and solar radiation data from the CRU were used as the independent variables, whereas the NDVI data from the GIMMS3g, which represent vegetation activities, were used as the dependent variables to evaluate their dependency at different time-lag scales. Previous studies found the time lag at the monthly scale of the vegetation responses to climate to generally be shorter than a quarter (Rundquist & Harrington, 2000; Anderson *et al.*, 2010; Chen *et al.*, 2014); therefore, this study considered the time lags for 0–3 months. The relationships between the NDVI and climatic factors are as shown in Eqns 1–3:

$$NDVI = k_i * TMP + b \quad (1)$$

$$NDVI = k_i * PRE + b \quad (2)$$

$$NDVI = k_i * SWD + b \quad (3)$$

where k_i refers to the regression coefficient with a time lag of i months; i ranges from 0 to 3 (i.e., 0 represents no time-lag effects, and 1–3 represents a 1–3 month lag, respectively); *NDVI* refers to the GIMMS3g NDVI time series (1982–2008); and *TMP*, *PRE*, and *SWD* are the time series for temperature, precipitation, and solar radiation, respectively, with a time lag of i. Statistical analysis in this study is based on the vegetation growing season, which is defined as those months with a

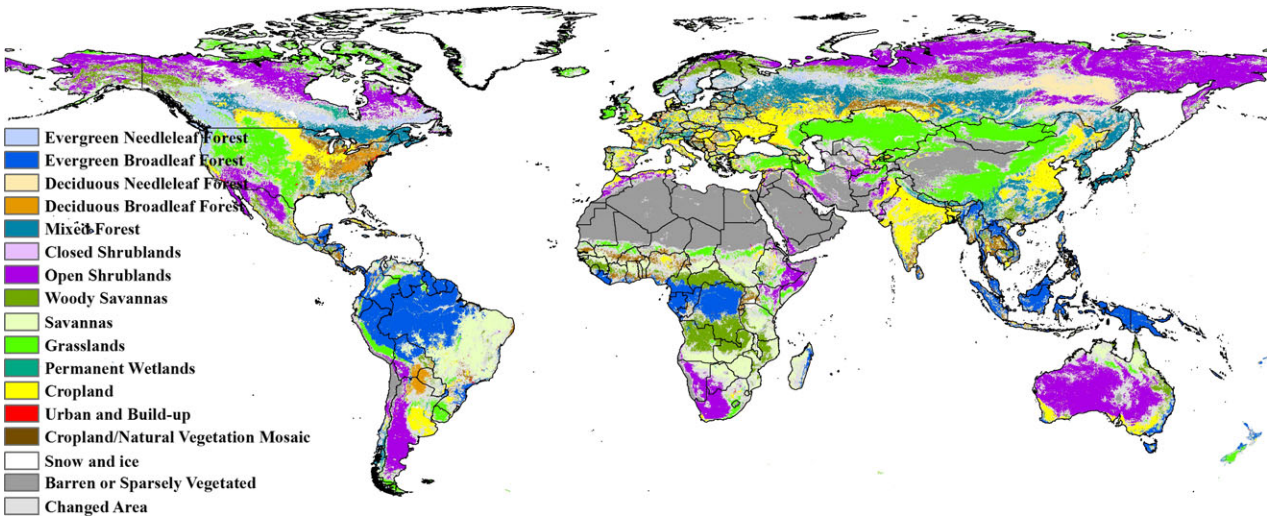

Fig. 1 Unchanged IGBP vegetation map of MCD12C1 from 2001 to 2008.

Table 1 MODIS IGBP vegetation types used in this study

No.	IGBP Land-cover Type
01	Evergreen needleleaf forest
02	Evergreen broadleaf forest
03	Deciduous needleleaf forest
04	Deciduous broadleaf forest
05	Mixed forest
N7	Open shrublands (North)
S7	Open shrublands (South)
08	Woody savannas
09	Savannas
10	Grasslands
12	Croplands
14	Cropland/natural vegetation mosaic

temperature higher than 0°C and a *NDVI* >0.2 in a year (Piao *et al*., 2006). For each climatic factor, the lag month (*i*) that has the highest determination coefficient (R^2) is the best time lag for the vegetation responses to this climatic factor.

Explanations of climatic factors on vegetation variation

A multiple linear regression model between the GIMMS3g NDVI and temperature, precipitation, and solar radiation was developed (Eqn 4), from which an explanation of all three climatic factors on vegetation variation was estimated:

$$NDVI = A * TMP_l + B * PRE_m + C * SWD_n + D + \varepsilon \quad (4)$$

where *l, m,* and *n* refer to the time lag of the vegetation to the three climatic factors, respectively; *NDVI* is the GIMMS3g NDVI time series data (1982–2008); *TMP, PRE,* and *SWD* are the time series data that correspond to temperature, precipitation, and solar radiation, respectively; *A, B,* and *C* are regression coefficients of multiple linear regression, respectively; and *D* is a constant and ε is error term.

Major climatic driving factors on vegetation growth

In consideration of the time-lag effects of the vegetation responses to different climatic factors, the partial correlation coefficient between the GIMMS3g NDVI and each climatic factor was calculated, with the other two climatic factors acting as control variables. The formula is as follows (Eqn 5):

$$r^2_{12,3\sim p} = \frac{R^2_{1(2,3,\ldots p)} - R^2_{1(3,\ldots p)}}{1 - R^2_{1(3,\ldots p)}} \quad (5)$$

where $r_{12,3\sim p}$ refers to the partial correlation coefficient of variables *1* and *2*; $R^2_{1(2,3,\ldots p)}$ is the determination coefficient of the regression analysis of variable *1* and variable (*2*~*p*); and $R^2_{1(3,\ldots p)}$ refers to the determination coefficient of the regression analysis of variable 1 and variable (*3*~*p*). For example, to calculate the partial correlation coefficient of NDVI to temperature, $r_{12,3\sim p}$ refers to the partial correlation coefficient of NDVI and temperature, which uses precipitation and radiation as control variables. $R^2_{1(2,3,\ldots p)}$ refers to the determination coefficient of the regression of NDVI, temperature, precipitation, and radiation; and $R^2_{1(3,\ldots p)}$ is the determination coefficient of the regression of NDVI and precipitation and radiation.

Global vegetation change under the climate-driving background in 1982–2008

Based on the identified vegetation responses to climatic factors, the climate-driving factors of vegetation that changed globally in 1982–2008 were further explored. Therefore, the changes of each factor in the growing seasons from 1982 to 2008 were evaluated based on the GIMMS3g NDVI data and the CRU temperature, precipitation, and radiation data, with corresponding month lags. The study adopted least squares to linearly fit the vegetation and climate time series data, and the result was tested at a significance level of 0.05. Spatial comparative analysis was conducted between significantly changed regions of global vegetation and climatic factors. According to the characteristics of the vegetation responses to climate, the causes for significant changes in regional vegetation and the major climate-driving factors were analyzed. All of the statistical analysis was performed pixel-by-pixel and tested at a significance level of 0.05.

Results

Time-lag effects of the global vegetation responses to climatic factors

The time-lag effects of the vegetation responses to the three climatic factors, that is, temperature, precipitation, and radiation, were obtained using GIMMS3g NDVI and CRU meteorological data with a long-time series (Fig. 2, Figs S1, S2, and Table S1). The results verified our hypothesis that different vegetation types have significantly different time-lag effects of vegetation responses to the same climatic factor, and the same vegetation type also shows significantly different lag effects of vegetation responses to different climatic factors.

Regarding the time-lag effects of vegetation to temperature at the global scale (Fig. 2a,d), the vegetation growth at the middle and high latitudes (30N–90N, 30S–90S) has the greatest correlation with temperature in the same month and does not exhibit apparent lag effects. The vegetation at low latitudes (30S–30N), however, exhibits a certain lag effects related to temperature, with the time lag in most regions exceeding one month. Most of the forest ecosystems do not show apparent lag effects to temperature. The grids of evergreen broadleaf forest, deciduous needleleaf forest, and mixed forest that do not have time-lag effects account for 62.97%, 100%, and 94.43% of the total grids, respectively. The average time lag is 0.82 (1.20 SD), 0.00 (0.00 SD), and 0.08 (0.39 SD) months, respectively. The evergreen needleleaf forest shows a longer time lag to temperature. The grids that have a 1-month time lag

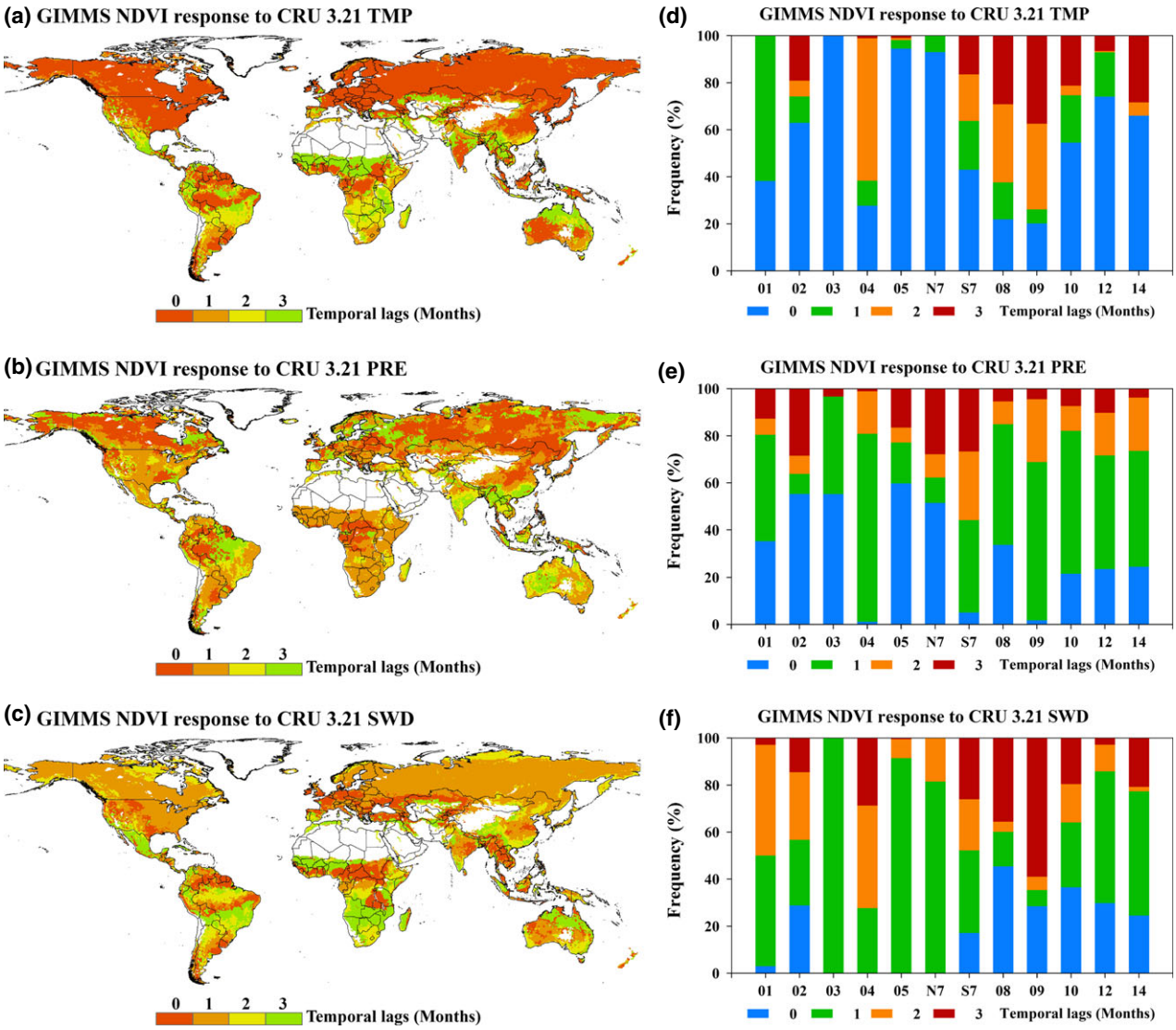

Fig. 2 Climatic factors' time lag at which the maximum correlation between GIMMS3g NDVI and climatic factors is found. Areas with no statistics are depicted in white. (a) Time lag of the GIMMS3g NDVI response to the CRU 3.21 temperature (TMP), (b) time lag of the GIMMS3g NDVI response to the CRU 3.21 precipitation (PRE), (c) time lag of the GIMMS3g NDVI response to the CRU 3.21 solar radiation (SWD), (d) frequency map of Figure 2a among vegetation types, (e) frequency map of Figure 2b among vegetation types, and (f) frequency map of Figure 2c among vegetation types. Vegetation types are introduced in Table 1.

account for 61.76% of the total grids, with an average time lag of 0.62 (0.49 SD). The deciduous broadleaf forest also exhibits the longer time lag to temperature. The grids of the 2-month time lag account for 60.64% of the total grids, with an average time lag of 1.35 (0.90 SD) months. The shrubs at different latitudes exhibit apparently different time lags to temperature. The shrubs located at high latitudes in the Northern Hemisphere exhibit the greatest correlation in the same month, with an average time lag of 0.07 (0.26 SD) months. The shrubs located at middle and low latitudes, however, have significantly different time-lag effects, with an average time lag of 1.10 (1.13 SD) months. Woody savanna and savanna are characterized by a consistent time lag to temperature, with average time lags of 1.70 (1.11 SD) and 1.91 (1.11 SD), respectively. The grassland grids have a response to the temperature in the same month that accounts for 54.55% of the total samples, with an average time lag of 0.92 (1.20 SD) months. The cropland grid has a response in the same month that accounts for 74.06%, with an average time lag of 0.39 (0.80 SD).

Among these cases, the temperature in the growing season decreases from the equator to the poles, whereas the demands of vegetation growth for ideal temperature conditions increase with latitude. Therefore, at the

middle and high latitudes in the Northern Hemisphere and the Qinghai–Tibet Plateau, most vegetation does not exhibit time-lag effects related to temperature, and the vegetation is significantly affected by the temperature in the same month. In the regions with relatively high temperatures during the growing season, the response of vegetation growth to temperature shows there are time-lag effects at a particular temporal scale. However, in some arid and semiarid regions (e.g., southern Australia and southern South America), vegetation does not exhibit time-lag effects to temperature and negatively correlated to the temperature, as the increasing temperature accelerates soil water evaporation and causes drought, thus inhibiting vegetation growth.

The time-lag effects of the vegetation responses to precipitation at the global scale (Fig. 2b,e) indicate that most of the vegetation at high northern latitudes has the greatest response within the same month (i.e., no apparent time-lag effects). The time lag in arid and semiarid areas, however, is approximately 1 month. This indicates the demand for water by regional vegetation in these areas. It also indicates that the vegetation growth in arid and semiarid areas is not primarily determined by the precipitation within the current month, but the previous month. Research in Kansas, USA, also demonstrated that the time lag of grassland ecosystems to precipitation was 1 month (Rundquist & Harrington, 2000). Considering the time-lag effects in that study, the correlation coefficient of the regional precipitation with NDVI increased by 0.3–0.4 compared to the result that did not consider the time-lag effects. That difference is consistent with the results in this study. The comparisons between shrubs at different latitudes indicated that shrubs at high latitudes have an average time lag of 1.14 (1.31 SD), whereas shrubs at low latitudes have a longer time lag of 1.78 (0.90 SD) months. Among other regions, the time-lag effects of precipitation have larger systematic differences and less obvious patterns.

With regard to the time-lag effects of the vegetation responses to solar radiation at the global scale (Fig. 2c, f), the time lag in most of the middle and high latitudes of the Northern Hemisphere is 1 month. This indicates that the radiation intensity in the previous month has important impacts on vegetation growth, possibly because the average radiation in the growing season in this area is relatively small compared with that in other regions and because vegetation growth requires more solar radiation for photosynthesis. The radiation in the previous month enables photosynthesis for carbon fixation, which provides the essential conditions for vegetation growth in the current month. The time lag of the deciduous needleleaf forest, mixed forest, and high-latitude shrubs is 1 month, with minor differences within ecosystems. The proportions of the pixels with the lag of 1 month are 100%, 91.24%, and 81.47%, respectively, and average time lags of 1.00 (0.00 SD), 1.09 (0.31 SD), and 1.19 (0.39 SD). Significant differences exist for the time lag in other areas and the time lags in most areas exceed 1 month.

Prediction based on a multiple linear regression model

Considering the time-lag effects, the relationship between climatic factors and vegetation growth at the global scale was established using a multiple linear regression model (Fig. 3, Figs S3, S4 and S5). Figure 3(a) illustrates the determination coefficient of the multiple linear regression model. Figure 3(b) shows the differences in climate contributions to vegetation growth, which was calculated by the models with and without the consideration of time-lag effects.

Results show that the average explanation of the three climatic factors to vegetation growth is 64.04% globally when the time-lag effects were considered. If the vegetation's lag effect is ignored, however, the average explanation is only 57.57% (Fig. 3a and Fig. S3), which is consistent with the results of Jong *et al.* (2013), whose explanation is 54.0%. In other words, the explanation of climate on vegetation growth will increase by 6.47% (i.e., relatively increase by 11.24%) if the model contains the time-lag effects at the global scale. The explanations for most vegetation types are 64–79%, and the model shows a good performance. However, for evergreen broadleaf forest and shrubs at middle and low latitudes, the explanation calculated for vegetation growth is lower, only 27% and 37%, respectively. For evergreen broadleaf forest, deciduous broadleaf forest, shrubs at middle and low latitudes, woody savannas, savannas, and croplands that show obvious time-lag effects, compared to the model that only considers the vegetation responses within the same month, the explanations of the improved model relatively increase by 21.56%, 47.44%, 54.34%, 14.22%, 46.46%, and 11.85% (Table S1), respectively. Therefore, the consideration of vegetation's time-lag effects to climatic factors provides a better understanding of vegetation growth response to climate, to a large extent.

Spatial patterns of climate-driven factors for global vegetation

Considering the time-lag effects of vegetation, the partial correlation coefficients of vegetation growth with temperature, precipitation, and solar radiation were also analyzed. Figure 4(a–c) and Fig. S6 show the partial correlation coefficients of temperature, precipitation, and

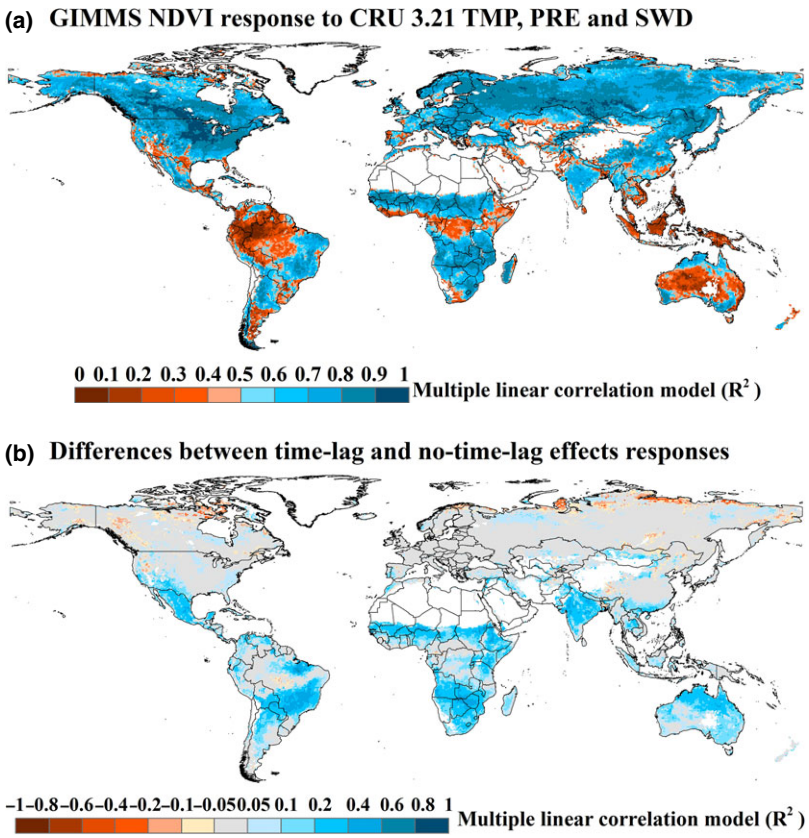

Fig. 3 Spatial patterns of the association observed between climatic factors and vegetation activity. (a) Spatial distribution of the determination coefficient (R^2) of the multiple linear regression model between the GIMMS3g NDVI and climatic factors for the period 1982–2008 with considering time-lag effects and (b) response differences of vegetation to climatic factors between the determination coefficient (R^2) considering time-lag effects or not.

solar radiation with vegetation and the corresponding significance of the partial correlation coefficients, respectively. The absolute value (0–1) of the partial correlation coefficient was obtained and then linearly stretched to 0–255; RGB synthesis was performed on the stretched values of temperature, precipitation, and solar radiation, and the result is shown in Fig. 4(d), which illustrates the major driving factors of climate on global vegetation growth.

The results indicate that the responses of vegetation growth to climate are primarily affected by temperature and radiation at high northern latitudes. In comparison, the eastern America is primarily affected by radiation, arid and semiarid regions at low latitudes are primarily affected by precipitation, and eastern China is affected primarily by temperature. As for tropical rainforest, there is no obvious regularity. Climatic factors can promote vegetation growth, but in some areas, the consequence is possibly the inverse. For example, for the Amazon rainforest, precipitation inhibits vegetation growth as higher precipitation generally signifies lower solar radiation and temperature. For the arid and semiarid areas in Western Australia, both temperature and radiation inhibit vegetation growth, as precipitation is a major constraint factor for vegetation growth.

The impacts of climate-driving factors on vegetation are also diverse for different vegetation types (Fig. 4a–c), and the major climate-driving factors for vegetation growth are closely related to the physical characteristics of plants and the corresponding climatic environment (Jong *et al.*, 2013). The growth of evergreen needleleaf forest, deciduous needleleaf forest, and mixed forest is driven by radiation and temperature, with the average partial correlation coefficients of 0.29 (0.21 SD) and 0.20 (0.15 SD), 0.28 (0.08 SD) and 0.47 (0.11 SD), and 0.29 (0.15 SD) and 0.41 (0.13 SD), respectively. The needleleaf forests are primarily distributed in middle and high latitudes in the Northern Hemisphere (Fig. 1), characterized by strong seasonal temperatures and solar radiation variations. Because of the weaker demand for water, these two climatic factors are the main climate-driven factors affecting the needleleaf forests' growth. Evergreen broadleaf forest is primarily distributed in tropical rainforests

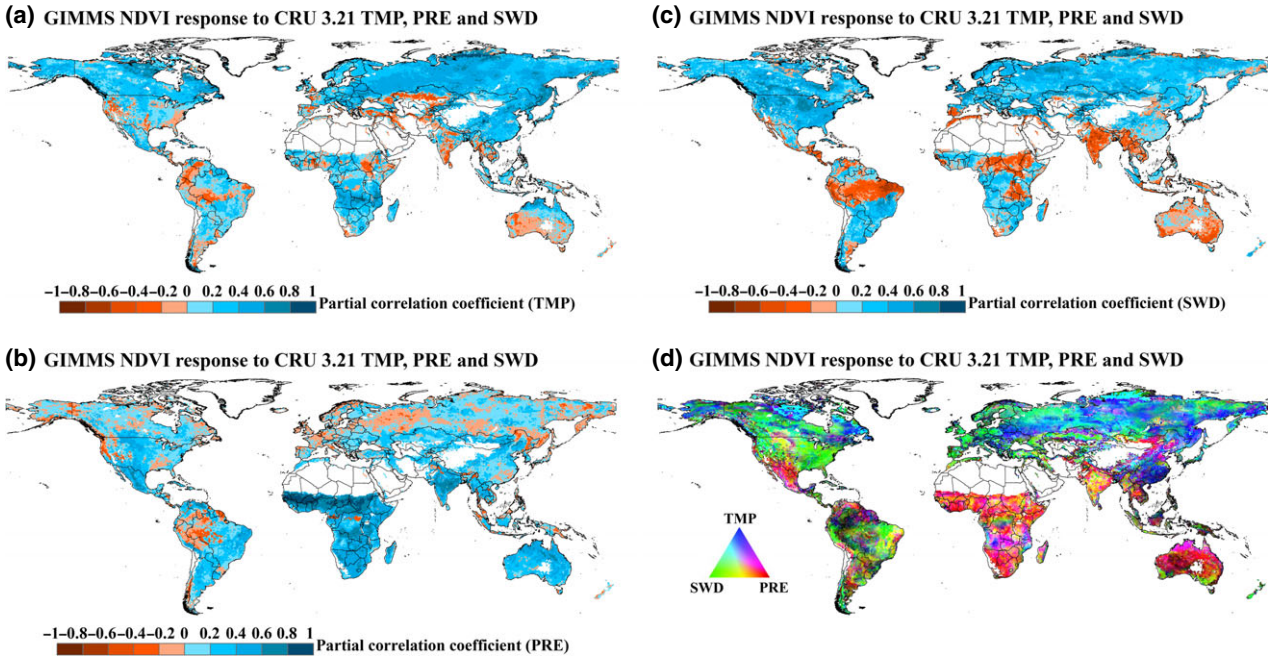

Fig. 4 The responses of the GIMMS3g NDVI to CRU temperature (TMP), precipitation (PRE), and solar radiation (SWD) considering time-lag effects. (a) Spatial distribution of the partial correlation coefficient between NDVI and temperature (TMP) after controlling for precipitation (PRE) and solar radiation (SWD), (b) spatial distribution of the partial correlation coefficient between NDVI and precipitation (PRE) after controlling for temperature (TMP) and solar radiation (SWD), (c) spatial distribution of the partial correlation coefficient between NDVI and solar radiation (SWD) after controlling for temperature (TMP) and precipitation (PRE), (d) spatial distribution of the main climate-driven factors to the vegetation growth derived from long-term statistics.

where the climatic conditions are moderate, thus the impacts of the three factors on vegetation growth are not significant in the model. Deciduous broadleaf forest is primarily distributed in middle latitudes where there is a higher demand for photosynthesis and water transpiration is quicker compared with coniferous forest. Thus, the growth of deciduous broadleaf forest is driven by radiation and precipitation, with average partial correlation coefficients of 0.21 (0.10 SD) and 0.40 (0.09 SD), respectively. The climate-driven factors for shrubs in northern high latitudes are radiation of 0.30 (0.24 SD) and temperature of 0.43 (0.20 SD). However, for shrubs at middle and low latitudes, both temperature and radiation are sufficient, whereas there is much less precipitation than other regions. As a result, rainfall is the major constraining factor to vegetation growth, with the average partial correlation coefficient of 0.36 (0.15 SD). The climate-driven factors for woody savannas are precipitation and temperature, with average partial correlation coefficients of 0.49 (0.23 SD) and 0.39 (0.21 SD), respectively. The major driving factor of climate for savannas is precipitation, with an average partial correlation coefficient of 0.47 (0.21 SD). Grasslands are primarily distributed in inland regions at middle latitudes, with relatively low precipitation. Sufficient photosynthesis and precipitation will promote growth, signifying that these two factors jointly determine the variation of grassland ecosystems, and the average partial correlation coefficients are 0.31 (0.27 SD) and 0.30 (0.18 SD), respectively. Croplands are jointly driven by all three climatic factors, precipitation, radiation, and temperature, with average partial correlation coefficients of 0.26 (0.21 SD), 0.16 (0.39 SD), and 0.17 (0.26 SD), respectively (Table S1). These results depict the specific spatial patterns of the climate-driven factors of vegetation growth globally, which provides a reference for understanding the reasons for vegetation growth driven by climate change.

Variation of vegetation driven by climate change in 1982–2008

To characterize the variation in global vegetation in the period 1982–2008 and to analyze its climate-driven factors, this study adopted a linear regression model to analyze the regions that have significant variation on vegetation growth during 1982–2008 (Fig. 5a). In addition, this study also analyzed the spatial patterns of the significant variations in global temperature, precipitation, and radiation during 1982–2008 (Figs S7 and S8). Figure 5(b) shows the comparison between climatic

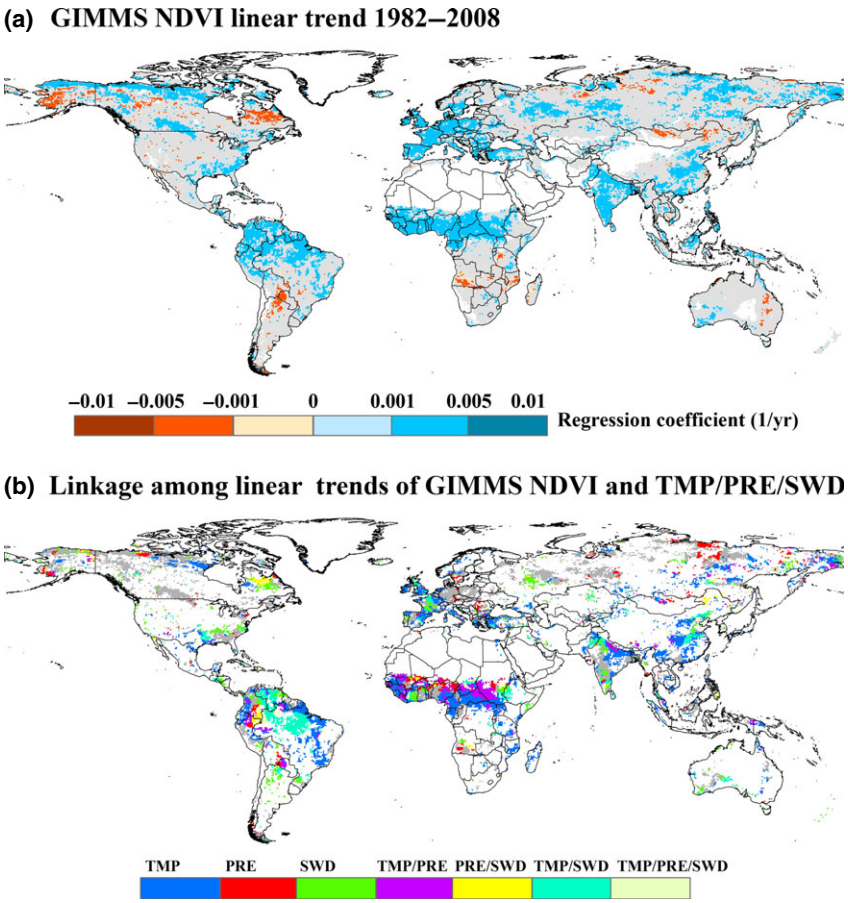

Fig. 5 (a) The GIMMS3g NDVI linear trend for the $P < 0.05$ significance level (1982–2008). (b) Comparison between climatic factors and vegetation in the areas with significant variation ($P < 0.05$).

factors and vegetation in the areas with significant variation ($P < 0.05$). The regions with a significant NDVI variation correspond to one significant changed climatic factor or multiple climatic factors.

The pixels with a significant temperature variation that correspond to a significant variation in the NDVI account for 45.09% of all pixels showing a significant NDVI variation, the pixels with a significant variation in precipitation account for 15.72%, and those with a significant variation in radiation account for 20.72%. The pixels showing significant variations in all three meteorological factors account for 60.66% of all pixels with a significant variation in the NDVI, signifying that climate changes control most of the vegetation changes. In the regions with significant variation in at least one climatic factor corresponding to a significant NDVI variation, the temperature ratio is the highest (74.33%), followed by radiation (34.16%) and precipitation (25.92%). Therefore, the explanation of temperature to vegetation growth is highest, and temperature variations are the major climatic-driven factors to vegetation change in the past 27 years.

Discussion

There are two major driving factors affecting vegetation growth. The first is climate-related factors (Peteet, 2000; Nemani *et al.*, 2003; Pearson *et al.*, 2013; Peng *et al.*, 2013), which provide necessary conditions for vegetation growth. The other is disturbance caused by both human activities and natural disturbances, such as agricultural irrigation, land-use change, forest development, fire, plant diseases, and pests (Bala *et al.*, 2007; Malhi *et al.*, 2008; Choat *et al.*, 2012; Sterling *et al.*, 2013; Brando *et al.*, 2014; Zhang & Liang, 2014). Because our study primarily focuses on plant growth responses to climatic factors in normal conditions, we do not quantitatively analyze the impacts of human activities and natural disturbances on regional vegetation growth.

Significant variation of global vegetation occurred from 1982 to 2008. The regions with a significant NDVI increase ($P < 0.05$) in the growing season account for 28.85% of the total statistical area, whereas the regions with a significant decrease ($P < 0.05$) account for 3.80%. The study shows that vegetation greenness in high

northern latitudes has increased continuously in the past 27 years (Fig. 5a) and the vegetation growth in these regions is primarily affected by temperature and radiation (Fig. 4d). Thus, an increase in temperature in high northern latitudes (Figs S7 and S8) is an important reason for the increase in vegetation greenness. Similarly, Jeong's study (Jeong *et al*., 2011) showed that climate warming resulted in an extended vegetation growing season in northern high latitudes, and an increase in vegetation greenness during the growing season. In central Africa, the major climate-driven factors on vegetation growth are precipitation and temperature (Fig. 4d). In Willis's study (Willis *et al*., 2013), an increase in temperature and moisture was shown to have resulted in greener vegetation in this region. By contrast, our study showed that temperature and precipitation increased during 1982–2008 (Figs S7 and S8), which confirms that the increase in vegetation greenness in this region is primarily caused by climate change. In central and eastern China, the NDVI has increased continuously over the past 27 years, and Fig. 4(d) shows that the major climate-driven factor in this region is temperature. Statistical results also show the temperature changed significantly in this region over the past 27 years (Figs S7 and S8), signifying that the NDVI increase in this region is primarily caused by temperature variation. This result is consistent with the studies conducted by Peng *et al.* (2011) and Piao *et al.* (2006), which indicated that an increase in temperature resulted in an extended growing season in northern China and an enhancement in vegetation activities during the growing season. Nemani *et al.* (2003) proposed in their study that the NPP increase of Amazon tropical rainforests was primarily caused by the decrease in cloud cover and increase in solar radiation. This study also shows a significant increase in temperature and solar radiation in this area during 1982–2008, thus these climatic variations might be one of the primarily reasons for increasing vegetation greenness.

In this study, we found that human activities and nature disturbances also play an important role in the variations of vegetation growth. The results from the study found that the vegetation in India is primarily affected by water condition (Fig. 4d). Thus, improving water conditions will increase the vegetation NDVI. Nayak *et al.* (2013) confirmed in their study that an increase in the NPP in this area from 1981 to 2006 was primarily caused by improved agricultural productivity. Our study also shows the vegetation greenness in India from 1982 to 2008 have increased continuously (Fig. 5a). Therefore, improved agricultural irrigation and regional water conditions in this area increased the vegetation greenness. In the eastern and southern America, the NDVI has increased significantly in the past 27 years, but the climatic factors in this area did not change significantly, the primary reason being effective forest management in recent years (including the growth of young trees and continuous afforestation) (Hicke *et al*., 2002). In eastern Canada, one of the reasons for the decrease in the vegetation NDVI is the increase in precipitation and decrease in radiation. Plant diseases and pests might be another reason (Hicke *et al*., 2002).

The normalized difference vegetation index in this work was used as an indicator to reveal the effects of climate factors and their time lag on vegetation's growth. As vegetation index represents the greenness of leaves and closely related with seasonal variation of vegetation photosynthesis (Peteet, 2000; Nemani *et al*., 2003; Pearson *et al*., 2013; Peng *et al*., 2013), it is sensitive to the climate factors and has the length of time lag at monthly scale (Rundquist & Harrington, 2000; Anderson *et al*., 2010; Chen *et al*., 2014). In addition to vegetation index, the radial growth of trees is another indicator that represents interannual variation of tree's growth and therefore extensively used to reveal the vegetation–climate interactions at yearly scale (Orwig & Abrams, 1997). Given that the radial growth reflects the balance of carbon influx through photosynthesis and efflux through respiration, its value depends on both climate factors and disturbances (Abrams & Nowacki, 2015a,b; Nowacki & Abrams, 2015) and has a relative longer time lag. For instance, the radial growth of trees is related with drought, with most trees exhibited growth reductions lasting 2–3 years (Orwig & Abrams, 1997). Similar result was revealed by Huang *et al.* (2015) who found that the radial growth of trees has a very good relationship with the standardized precipitation evapotranspiration index (SPEI) at time scale of 11 months. The relative longer time lag in radial growth indicated that the factors impacting carbon balance are more complicated than those impacting only leaves variation.

Throughout this work, we analyzed the time-lag effects of vegetation responses to climatic factors with GIMMS3g NDVI data and CRU climate data and revealed the effects of time lag on the explanations of climatic factors, identifying the major driving factors for the different vegetation types and the regions associated with significant vegetation and climate variations during the period 1982–2008.

Our results show that (i) the same type of vegetation has different time-lag effects from different climatic factors, and different vegetation types respond differently to the same climatic factor; (ii) consideration of the time-lag effects of vegetation is very important for accurately revealing the response of vegetation growth to climatic factors. In general, the three climatic indicators

explain 64.04% of the vegetation growth globally. When the time-lag effects are considered, the explanation relatively increases by 11.24%, particularly for the open shrubs at middle and low latitudes where the value relatively increases by 54.34%. In other words, the studies on vegetation responses to climate should not ignore the time-lag effects; (iii) the major climate-driven factors for vegetation growth are diverse and are closely related to the vegetation characteristics and climatic condition; and (iv) the results at the global scale indicated that temperature is the major driving factor, which accounts for 45.09% of the spatial grids that show significant variation in the NDVI. As a comparison, precipitation and radiation account for 15.72% and 20.72% of the grids, respectively. This study reveals that vegetation growth for certain regions is also related with natural or human disturbances. However, this study focuses on the impacts of climatic factors at the global scale and, therefore, does not quantitatively analyze these nonclimatic factors. Overall, this study provides a theoretical basis for revealing the spatial patterns and time-lag effects of global vegetation responses to climate, and the results hold significant value for the climate-based prediction of variations in vegetation growth in the future.

Acknowledgements

This work was supported by the High Technology Research and Development Program of China (Grant No. 2013AA122801), National Natural Science Foundation of China (Grant No. 41331173 and 41301353), the Fund for Creative Research Groups of National Natural Science Foundation of China (Grant No. 41321001) and Fundamental Research Funds for the Central Universities (Grant No. 2014KJJCB17).

References

Abrams MD, Nowacki GJ (2015a) Exploring the early anthropocene burning hypothesis and climate-fire anomalies for the Eastern U.S. *Journal of Sustainable Forestry*, **34**, 30–48.

Abrams MD, Nowacki GJ (2015b) Large-scale catastrophic disturbance regimes can mask climate change impacts on vegetation-a reply to Pederson et al. (2014). *Global Change Biology*, doi: 10.1111/gcb.12828.

Anderson LO, Malhi Y, Aragão LEOC, Ladle R, Arai E, Barbier N, Phillips O (2010) Remote sensing detection of droughts in Amazonian forest canopies. *New Phytologist*, **187**, 733–750.

Arnone Iii JA, Verburg PSJ, Johnson DW *et al.* (2008) Prolonged suppression of ecosystem carbon dioxide uptake after an anomalously warm year. *Nature*, **455**, 383–386.

Bala G, Caldeira K, Wickett M, Phillips TJ, Lobell DB, Delire C, Mirin A (2007) Combined climate and carbon-cycle effects of large-scale deforestation. *Proceedings of the National Academy of Sciences*, **104**, 6550–6555.

Beer C, Reichstein M, Tomelleri E *et al.* (2010) Terrestrial gross carbon dioxide uptake: global distribution and covariation with climate. *Science*, **329**, 834–838.

Bonan GB (2008) Forests and climate change: forcings, feedbacks, and the climate benefits of forests. *Science*, **320**, 1444–1449.

Brando PM, Balch JK, Nepstad DC *et al.* (2014) Abrupt increases in Amazonian tree mortality due to drought–fire interactions. *Proceedings of the National Academy of Sciences*, **111**, 6347–6352.

Braswell B, Schimel D, Linder E, Moore B (1997) The response of global terrestrial ecosystems to interannual temperature variability. *Science*, **278**, 870–873.

Chen T, RaM De Jeu, Liu YY, Van Der Werf GR, Dolman AJ (2014) Using satellite based soil moisture to quantify the water driven variability in NDVI: a case study over mainland Australia. *Remote Sensing of Environment*, **140**, 330–338.

Choat B, Jansen S, Brodribb TJ *et al.* (2012) Global convergence in the vulnerability of forests to drought. *Nature*, **491**, 752–755.

Craine JM, Nippert JB, Elmore AJ, Skibbe AM, Hutchinson SL, Brunsell NA (2012) Timing of climate variability and grassland productivity. *Proceedings of the National Academy of Sciences*, **109**, 3401–3405.

Davis M (1989) Lags in vegetation response to greenhouse warming. *Climatic Change*, **15**, 75–82.

De Jong R, Verbesselt J, Zeileis A, Schaepman M (2013) Shifts in global vegetation activity trends. *Remote Sensing*, **5**, 1117–1133.

Easterling DR, Meehl GA, Parmesan C, Changnon SA, Karl TR, Mearns LO (2000) Climate extremes: observations, modeling, and impacts. *Science*, **289**, 2068–2074.

Fensholt R, Proud SR (2012) Evaluation of Earth Observation based global long term vegetation trends-Comparing GIMMS and MODIS global NDVI time series. *Remote Sensing of Environment*, **119**, 131–147.

Friedl MA, Mciver DK, Hodges JCF *et al.* (2002) Global land cover mapping from MODIS: algorithms and early results. *Remote Sensing of Environment*, **83**, 287–302.

Friedl MA, Sulla-Menashe D, Tan B, Schneider A, Ramankutty N, Sibley A, Huang X (2010) MODIS Collection 5 global land cover: algorithm refinements and characterization of new datasets. *Remote Sensing of Environment*, **114**, 168–182.

Friedman J, Hastie T, Tibshirani R (2000) Additive logistic regression: a statistical view of boosting (With discussion and a rejoinder by the authors). *Annals of Statistics*, **28**, 337–407.

Harris I, Jones P, Osborn T, Lister D (2014) Updated high-resolution grids of monthly climatic observations-the CRU TS3. 10 Dataset. *International Journal of Climatology*, **34**, 623–642.

Hicke JA, Asner GP, Randerson JT *et al.* (2002) Trends in North American net primary productivity derived from satellite observations, 1982–1998. *Global Biogeochemical Cycles*, **16**, 2-1–2-14.

Holben BN (1986) Characteristics of maximum-value composite images from temporal AVHRR data. *International Journal of Remote Sensing*, **7**, 1417–1434.

Huang K, Yi C, Wu D *et al.* (2015) Tipping point of a conifer forest ecosystem under severe drought. *Environmental Research Letters*, **10**. doi: 10.1088/1748-9326/10/2/024011.

Jeong S-J, Ho C-H, Gim H-J, Brown ME (2011) Phenology shifts at start vs. end of growing season in temperate vegetation over the Northern Hemisphere for the period 1982–2008. *Global Change Biology*, **17**, 2385–2399.

Jones P, Lister D, Osborn T, Harpham C, Salmon M, Morice C (2012) Hemispheric and large-scale land-surface air temperature variations: an extensive revision and an update to 2010. *Journal of Geophysical Research: Atmospheres*, **1984–2012**, 117.

Jong R, Schaepman ME, Furrer R, Bruin S, Verburg PH (2013) Spatial relationship between climatologies and changes in global vegetation activity. *Global Change Biology*, **19**, 1953–1964.

Karl TR, Trenberth KE (2003) Modern global climate change. *Science*, **302**, 1719–1723.

Kelly AE, Goulden ML (2008) Rapid shifts in plant distribution with recent climate change. *Proceedings of the National Academy of Sciences*, **105**, 11823–11826.

Kumar P (2013) Hydrology: seasonal rain changes. *Nature Climate Change*, **3**, 783–784.

Kuzyakov Y, Gavrichkova O (2010) REVIEW: time lag between photosynthesis and carbon dioxide efflux from soil: a review of mechanisms and controls. *Global Change Biology*, **16**, 3386–3406.

Lewis SL, Brando PM, Phillips OL, Van Der Heijden GMF, Nepstad D (2011) The 2010 Amazon drought. *Science*, **331**, 554.

Malhi Y, Roberts JT, Betts RA, Killeen TJ, Li W, Nobre CA (2008) Climate change, deforestation, and the fate of the Amazon. *Science*, **319**, 169–172.

Mao J, Shi X, Thornton P, Hoffman F, Zhu Z, Myneni R (2013) Global latitudinal-asymmetric vegetation growth trends and their driving mechanisms: 1982–2009. *Remote Sensing*, **5**, 1484–1497.

Marengo JA, Nobre CA, Tomasella J *et al.* (2008) The drought of Amazonia in 2005. *Journal of Climate*, **21**, 495–516.

Mitchell TD, Jones PD (2005) An improved method of constructing a database of monthly climate observations and associated high-resolution grids. *International Journal of Climatology*, **25**, 693–712.

Nayak RK, Patel NR, Dadhwal VK (2013) Inter-annual variability and climate control of terrestrial net primary productivity over India. *International Journal of Climatology*, **33**, 132–142.

Nemani RR, Keeling CD, Hashimoto H *et al*. (2003) Climate-driven increases in global terrestrial net primary production from 1982 to 1999. *Science*, **300**, 1560–1563.
New M, Hulme M, Jones P (2000) Representing twentieth-century space-time climate variability. Part II: development of 1901–96 monthly grids of terrestrial surface climate. *Journal of Climate*, **13**, 2217–2238.
Nowacki GJ, Abrams MD (2015) Is climate an important driver of post-European vegetation change in the Eastern United States? *Global Change Biology*, **21**, 314–334.
Orwig DA, Abrams MD (1997) Variation in radial growth responses to drought among species, site, and canopy strata. *Trees*, **11**, 474–484.
Pearson RG, Phillips SJ, Loranty MM, Beck PSA, Damoulas T, Knight SJ, Goetz SJ (2013) Shifts in Arctic vegetation and associated feedbacks under climate change. *Nature Climate Change*, **3**, 673–677.
Peng S, Chen A, Xu L *et al.* (2011) Recent change of vegetation growth trend in China. *Environmental Research Letters*, **6**. doi: 10.1088/1748-9326/6/4/044027.
Peng S, Piao S, Ciais P *et al.* (2013) Asymmetric effects of daytime and night-time warming on Northern Hemisphere vegetation. *Nature*, **501**, 88–92.
Peteet D (2000) Sensitivity and rapidity of vegetational response to abrupt climate change. *Proceedings of the National Academy of Sciences*, **97**, 1359–1361.
Piao S, Fang J, Zhou L, Ciais P, Zhu B (2006) Variations in satellite-derived phenology in China's temperate vegetation. *Global Change Biology*, **12**, 672–685.
Rammig A, Wiedermann M, Donges J *et al.* (2014) Tree-ring responses to extreme climate events as benchmarks for terrestrial dynamic vegetation models. *Biogeosciences Discussions*, **11**, 2537–2568.
Reichstein M, Bahn M, Ciais P *et al.* (2013) Climate extremes and the carbon cycle. *Nature*, **500**, 287–295.
Rundquist BC, Harrington JA Jr (2000) The effects of climatic factors on vegetation dynamics of tallgrass and shortgrass cover. *GeoCarto International*, **15**, 33–38.
Saatchi S, Asefi-Najafabady S, Malhi Y, Aragão LEOC, Anderson LO, Myneni RB, Nemani R (2013) Persistent effects of a severe drought on Amazonian forest canopy. *Proceedings of the National Academy of Sciences*, **110**, 565–570.
Sterling SM, Ducharne A, Polcher J (2013) The impact of global land-cover change on the terrestrial water cycle. *Nature Climate Change*, **3**, 385–390.
Tucker CJ, Pinzon JE, Brown ME *et al.* (2005) An extended AVHRR 8-km NDVI dataset compatible with MODIS and SPOT vegetation NDVI data. *International Journal of Remote Sensing*, **26**, 4485–4498.
Vicente-Serrano SM, Gouveia C, Camarero JJ *et al.* (2012) Response of vegetation to drought time-scales across global land biomes. *Proceedings of the National Academy of Sciences*, **110**, 52–57.
Walther G-R, Post E, Convey P *et al.* (2002) Ecological responses to recent climate change. *Nature*, **416**, 389–395.
Wang X, Piao S, Ciais P, Li J, Friedlingstein P, Koven C, Chen A (2011) Spring temperature change and its implication in the change of vegetation growth in North America from 1982 to 2006. *Proceedings of the National Academy of Sciences*, **108**, 1240–1245.
Willis KJ, Bennett KD, Burrough SL, Macias-Fauria M, Tovar C (2013) Determining the response of African biota to climate change: using the past to model the future. *Philosophical Transactions of the Royal Society B: Biological Sciences*, **368**. doi: 10.1098/rstb.2012.0491.
Wu D, Wu H, Zhao X, Zhou T, Tang B, Zhao W, Jia K (2014) Evaluation of spatiotemporal variations of global fractional vegetation cover based on GIMMS NDVI Data from 1982 to 2011. *Remote Sensing*, **6**, 4217–4239.
Xu L, Samanta A, Costa MH, Ganguly S, Nemani RR, Myneni RB (2011) Widespread decline in greenness of Amazonian vegetation due to the 2010 drought. *Geophysical Research Letters*, **38**. doi: 10.1029/2011GL046824.
Zhang Y, Liang S (2014) Changes in forest biomass and linkage to climate and forest disturbances over Northeastern China. *Global Change Biology*, **20**, 2596–2606.
Zhang X, Susan Moran M, Zhao X, Liu S, Zhou T, Ponce-Campos GE, Liu F (2014) Impact of prolonged drought on rainfall use efficiency using MODIS data across China in the early 21st century. *Remote Sensing of Environment*, **150**, 188–197.
Zhao M, Running SW (2010) Drought-induced reduction in global terrestrial net primary production from 2000 Through 2009. *Science*, **329**, 940–943.
Zhou L, Tian Y, Myneni RB *et al.* (2014) Widespread decline of Congo rainforest greenness in the past decade. *Nature*, **509**, 86–90.

Supporting Information

Additional Supporting Information may be found in the online version of this article:

Figure S1. Correlation coefficient (R) at which the maximum correlation between climatic factors and the GIMMS3g NDVI is found.
Figure S2. Significance of the correlation coefficient (R) at which the maximum correlation between climatic factors and the GIMMS3g NDVI is found.
Figure S3. Spatial patterns of the determination coefficient (R^2) of the multiple linear regression model between the GIMMS3g NDVI and climatic factors for the period 1982–2008 without considering time-lag effects.
Figure S4. Spatial patterns of the multiple linear regression coefficient between climatic factors and the GIMMS3g NDVI with considering time-lag effects.
Figure S5. Spatial patterns of the significance of multiple linear regression coefficient between climatic factors and the GIMMS3g NDVI with considering time-lag effects.
Figure S6. Geographical patterns of the significance of partial correlation coefficient observed between climatic factors and the GIMMS3g NDVI with considering time-lag effects.
Figure S7. Linear trends of the climatic factors during the period 1982–2008 considering time-lag effects.
Figure S8. Significance of the linear trends of the climatic factors during the period 1982–2008 considering time-lag effects.
Table S1. Mean and standard deviation (SD) of the statistical parameters among the different vegetation types.